OPEN

Linear structural evolution induced tunable photoluminescence in clinopyroxene solid-solution phosphors

Zhiguo Xia[1], Yuanyuan Zhang[1], Maxim S. Molokeev[2], Victor V. Atuchin[3] & Yi Luo[1]

[1]School of Materials Sciences and Technology, China University of Geosciences, Beijing 100083, China, [2]Laboratory of Crystal Physics, Institute of Physics, SB RAS, Krasnoyarsk 660036, Russia, [3]Laboratory of Optical Materials and Structures, Institute of Semiconductor Physics, SB RAS, Novosibirsk 630090, Russia.

Clinopyroxenes along the Jervisite ($NaScSi_2O_6$) – Diopside ($CaMgSi_2O_6$) join have been studied, and a solid-solution of the type $(Na_{1-x}Ca_x)(Sc_{1-x}Mg_x)Si_2O_6$ has been identified in the full range of $0 \leq x \leq 1$. The powder X-ray patterns of all the phases indicate a structural similarity to the end compounds and show smooth variation of structural parameters with composition. The linear structural evolution of iso-structural $(Na_{1-x}Ca_x)(Sc_{1-x}Mg_x)Si_2O_6$ solid-solutions obeying Vegard's rule has also been examined and verified by high resolution transmission electron microscopy (HRTEM). The continuous solid-solutions show the same structural type, therefore the photoluminescence spectra of Eu^{2+} doped samples possess the superposition of spectral features from blue-emitting component ($CaMgSi_2O_6$:Eu^{2+}) and yellow-emitting one ($NaScSi_2O_6$:Eu^{2+}). This indicates that the spectroscopic properties of $(Na_{1-x}Ca_x)(Sc_{1-x}Mg_x)Si_2O_6$ clinopyroxene solid-solutions are in direct relations with structural parameters, and it is helpful for designing color-tunable photoluminescence with predetermined parameters.

White light-emitting diodes (w-LEDs) lighting can offer many benefits, and nowadays phosphor-converted w-LEDs utilizing phosphors to convert the radiation of a near-UV or blue LED chip into white light are paid more attentions[1,2]. Although yellow-emitting $Y_3Al_5O_{12}$:Ce^{3+} based phosphors pumped by blue LEDs are commercial available, however, low color rendering index and high color temperature for the lack of sufficient red emission restrict its wide application[3]. As an improved way, three-band w-LEDs with excellent light quality were proposed by the combination of the blue-emitting GaN-based LED with green and red phosphors, or pumping tricolor phosphors with near-UV or violet LED[4–6]. Alternatively, it is also an excellent strategy to develop a single-phase white-emitting phosphor[7–10], and the conventional single-phase white phosphors were designed with the codoped tricolor emitting activator ions and the energy transfer among them, such as Eu^{2+}-Mn^{2+} system[7], Ce^{3+}-Mn^{2+} system[8], Eu^{2+}-Tb^{3+}-Mn^{2+} system[9], Ce^{3+}-Tb^{3+}-Mn^{2+} system[10], and so on. However, the investigations on single-doped activator with full-color-emitting phosphors were rarely reported. Such a way can be principally realized by designing the activator ions entering different crystallographic sites and showing corresponding full-color emission in the single host system. Herein we reveal a new approach to realizing the color-tunable photoluminescence through spectral mixing in the composition-controlled solid-solution system, as reported in the present study of iso-structural clinopyroxene solid-solution phosphors $(Na_{1-x}Ca_x)(Sc_{1-x}Mg_x)Si_2O_6$:$Eu^{2+}$.

Pyroxenes belong to the group of chain silicates with the general formula {M2}[M1]T_2O_6. The mineral group of the pyroxenes shows rich crystal chemistry due to the wide range of possible cationic substitutions. Their possible space groups are $C2/c$, $P2_1/c$ and $P2/n$ depending on their chemical composition and genetic history, in which monoclinic pyroxenes forming in the $C2/c$ structures are called clinopyroxenes[11]. In the course of the present investigation, we report on the binary solid-solution series of Jervisite ($NaScSi_2O_6$) – Diopside ($CaMgSi_2O_6$) with a coupled Na^+—Ca^{2+} and Sc^{3+}—Mg^{2+} substitution. The Ca-rich clinopyroxene—diopside with ideal end-member composition of $CaMgSi_2O_6$ is an important component of both mafic and ultramafic rocks, and $CaMgSi_2O_6$:Eu^{2+} has been previously proposed as a blue-color phosphor (with peak emission at ~449 nm)[12]. $NaScSi_2O_6$:Eu^{2+} has been recently developed in our group as a new yellow-emitting phosphor with peak at 532 nm[13]. Since the two phosphor systems show blue and yellow emission, color-tunable photoluminescence and even the single-phase white phosphors can be expected among them. However, no detailed structural

investigations have been produced so far along this solid-solution series, and no studies of photoluminescence properties in $(Na_{1-x}Ca_x)(Sc_{1-x}Mg_x)Si_2O_6:Eu^{2+}$ have been reported.

Results

Determination and evidence of linear structural evolution. The chemical composition of the samples can be generalized as $(Na_{1-x}Ca_x)(Sc_{1-x}Mg_x)Si_2O_6:0.03Eu^{2+}$ ($0 \leq x \leq 1$). The XRD patterns recorded from the $(Na_{1-x}Ca_x)(Sc_{1-x}Mg_x)Si_2O_6:0.03Eu^{2+}$ ($x = 0, 0.2, 0.4, 0.6, 0.8$ and 1.0) solid-solution can be very well refined as the one-phase patterns, corresponding to any one of the JCPDS card files of $NaScSi_2O_6$ (JCPDS, 82-0532), $a = 9.8372(10)$, $b = 9.0550(5)$, $c = 5.3488(6)$ Å, $\beta = 107.175(5)°$, $V = 455.20(4)$ Å³ and $CaMgSi_2O_6$ (JCPDS, 78-1390), $a = 9.751(3)$, $b = 8.931(3)$, $c = 5.255(2)$ Å, $\beta = 105.89(3)°$, $V = 440.2(2)$ Å³, (Supporting Information, Figure S1)[14,15]. In order to further examine the phase purity and cation site occupancy in the solid-solution phosphors at each composition of $x = 0, 0.2, 0.4, 0.6, 0.8$ and 1.0, the respective Rietveld difference plots and the fractional atomic coordinates and isotropic or equivalent isotropic displacement parameters were defined, which are given in the supporting information (Figure S2–S7 and Table S1–S6). The main parameters of processing and refinement of the $(Na_{1-x}Ca_x)(Sc_{1-x}Mg_x)Si_2O_6:0.03Eu^{2+}$ solutions are given in Table S7. It is found that the refined x values are in good relation with nominal x values taken in the designed compositions. Furthermore, there are no additive superstructure peaks observed in the XRD patterns, and this indicates the absence of Na/Ca and Mg/Sc ordering. Thus, the ions are randomly mixed at atomic level. As a further examination of the utility of the Na^+/Ca^{2+} and Sc^{3+}/Mg^{2+} substitutions, the unit cell parameters (a, b, c and V) of solid-solution series obtained from Rietveld analysis are given in Figure 1. All the three unit cell parameters and unit cell volume are proportional to x value, which also verified that the solutions are iso-structural. There are not any structural kinks over the composition range of $0 \leq x \leq 1$. It is the most interesting to find that the parallel substitution in two cation sublattice obeys excellent Vegard's rule for structural parameters with the linear fitting factors (R^2) in the range of 0.9949–0.9976[16].

According to linear structural evolution, solid-solution phosphor with composition of $(Na_{0.7}Ca_{0.3})(Sc_{0.7}Mg_{0.3})Si_2O_6:0.03Eu^{2+}$ was selected, and its structure was carefully refined (Figure 2). There is no impurity peaks detected in the pattern, and it is iso-structural to $CaMgSi_2O_6$ and $NaScSi_2O_6$ compounds as discussed above. Furthermore, as an example, we have also refined the Eu^{2+} sites in $(Na_{0.7}Ca_{0.3})(Sc_{0.7}Mg_{0.3})Si_2O_6$ system. It is proposed that the model $(Ca_{0.97x}Na_{0.97(1-x)}Eu_{0.03})(Mg_xSc_{1-x})SiO_6$ should be in good relation with effective ion radii system earlier obtained for oxides. As it appeared, the Sc/Mg sites are very small for Eu^{2+} ion. Indeed, ion radii $R(Sc^{3+}_{CN=6}) = 0.745$ Å, $R(Mg^{2+}_{N=6}) = 0.72$ Å, $R(Na^{1+}_{CN=8}) = 1.18$ Å, $R(Ca^{2+}_{N=8}) = 1.12$ Å and $R(Eu^{2+}_{CN=6-8}) = 1.17$–$1.25$ Å[17]. One can see that Eu^{2+} ion can be much easier accommodated at the Na/Ca site than at the Mg/Sc one. Therefore, the preferred crystallographic positions of Eu^{2+} ions were refined and further verified on the basis of Rietveld analysis, a similar work on the Eu^{2+} sites occupancy in this structure has also been analyzed in detail and reported recently[13]. As given in Table S8, the main parameters of processing and refinement of $(Na_{0.7}Ca_{0.3})(Sc_{0.7}Mg_{0.3})Si_2O_6:0.03Eu^{2+}$ sample were given. The fractional atomic coordinates and isotropic or equivalent isotropic displacement parameters are demonstrated in Table S9. It was concluded that the structure model of $(Na_{0.671(6)}Ca_{0.300(6)}Eu_{0.03})(Sc_{0.691(6)}Mg_{0.309(6)})Si_2O_6$ is the best one. This model yields low R-factors and normal thermal parameters of all atoms (Table S9). The obtained unit cell parameters of this selected sample ($x = 0.3$) can also verify the linear structural evolution in the iso-structural $(Na_{1-x}Ca_x)(Sc_{1-x}Mg_x)Si_2O_6$ solid-solution. It is well known that the structure of pyroxenes can be described in terms of alternating tetrahedral and octahedral layers that lie parallel to the (100)-plane. The
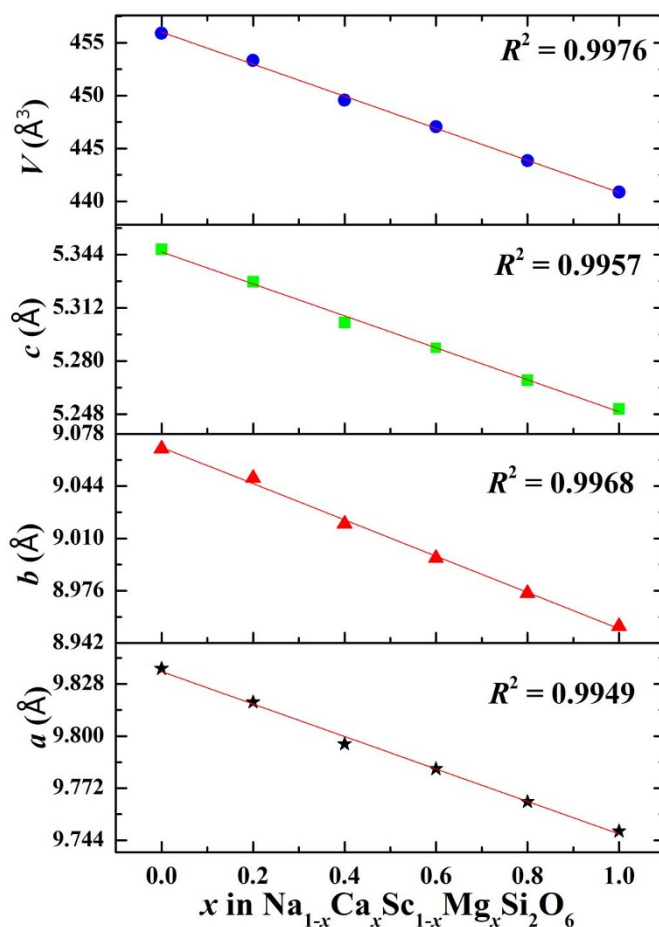
Figure 1 | Variation of unit cell parameters (a, b, c and V) of $Na_{1-x}Ca_x)(Sc_{1-x}Mg_x)Si_2O_6:0.03Eu^{2+}$ solid-solution series dependent on x values.

crystal structure of $CaMgSi_2O_6$ is of space group $C2/c$, and the M1 and M2 sites are occupied by Mg and Ca, respectively. The crystal structure of $NaScSi_2O_6$ is iso-morphous with that of $CaMgSi_2O_6$, and the octahedral M1 site is occupied by Sc and M2 by Na[18]. As it was discussed above, $NaScSi_2O_6$ and $CaMgSi_2O_6$ can form a complete series of solid-solutions. In the solutions, the replacement of Mg^{2+} by Sc^{3+} in the M1 site is strongly accompanied by a Ca^{2+} replacement by Na^+ in the M2 site, to assure the charge balance. The polyhedral representation of the structure of $(Na_{0.7}Ca_{0.3})(Sc_{0.7}Mg_{0.3})Si_2O_6:0.03Eu^{2+}$ solid-solution, and both the co-existing $(Sc/Mg)O_6$ octahedra and (SiO_4) tetrahedra are shown in the inset of Figure 2. In this structure, the cations of Na^+, Ca^{2+} and Eu^{2+} possess the same crystallographic positions.

Coexistence and the element distribution of Na, Sc, Ca, Mg, Si and O in the solid-solution series was examined and verified by the HRTEM and the corresponding Energy Dispersive X-ray Spectrometry (EDS) analysis as shown in Figure 3a–b. Figure 3a shows the TEM image obtained from the selected solid-solution crystal of reprehensive composition with $x = 0.4$, and all the elements can be detected in the solid-solution from one complete microcrystal sample (red square region) (Figure 3b). The fine structures of typical $(Na_{1-x}Ca_x)(Sc_{1-x}Mg_x)Si_2O_6:Eu^{2+}$ solid-solution phosphor samples are further examined by HRTEM and fast Fourier transform (FFT) images as show in Figure 3c–f suggesting the different selected compositions ($x = 0$ for Figure 3c, $x = 0.4$ for Figure 3d, $x = 0.8$ for Figure 3e and $x = 1$ for Figure 3f). Both of the HRTEM and FFT patterns recorded for the selected samples indicated that there were not significant structural defects in these single-phase samples and
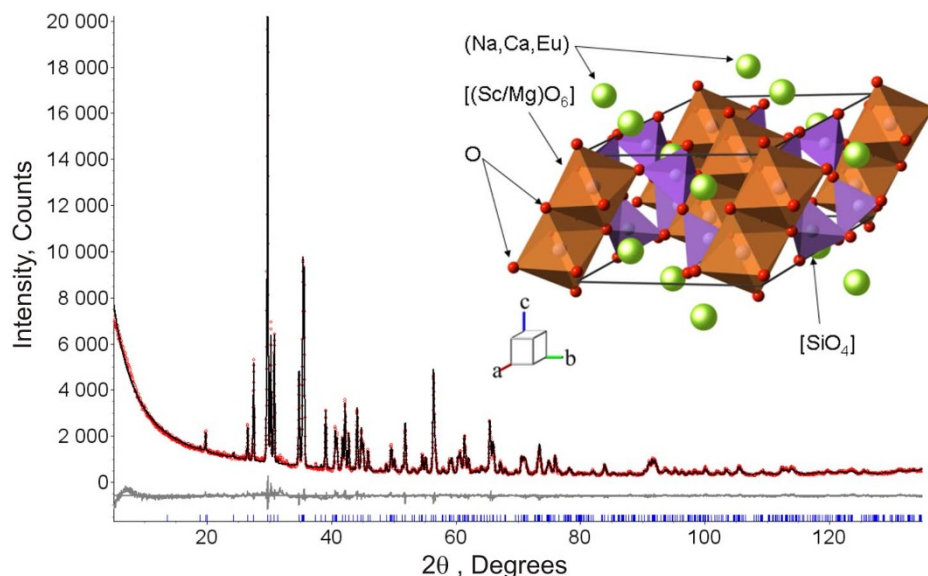
Figure 2 | Powder XRD patterns for Rietveld structure analysis of the selected $(Na_{1-x}Ca_x)(Sc_{1-x}Mg_x)Si_2O_6:0.03Eu^{2+}$ ($x = 0.3$) sample. The inset gives the polyhedral representation of the structure of solid-solution sample, and the (Na, Ca, Eu) position and the co-existing $[(Sc/Mg)O_6]$ octahedra and $[SiO_4]$ tetrahedra are shown in it.

confirmed the highly single-crystalline nature. It could be seen in Figure 3 (d) and 3(f) that the continuous lattice fringes measurements with d spacings of 0.458 nm and 0.362 nm could be assigned to the corresponding (020) and (111) planes with conventional d spacing 0.452 nm for $NaScSi_2O_6$ or 0.447 nm for $CaMgSi_2O_6$ and 0.366 nm for $CaMgSi_2O_6$ or 0.367 for $NaScSi_2O_6$. From the above discussion on XRD analysis, the behavior of structural parameters in the $(Na_{1-x}Ca_x)(Sc_{1-x}Mg_x)Si_2O_6$ ($0 \leq x \leq 1$) solid-solutions is in line with Vegard's rule. Therefore, we tried to find the similar relationship in the microstructure. Accordingly, we could transfer the measured d spacings in different orientation into the same d spacing value of [020] based on the classic Bragg equation[19]. As is shown in Figure 3c–f, d-spacings of the principal planes are about 0.304 nm corresponding to ($\bar{2}21$), 0.336 nm corresponding to (021) and 0.362 nm corresponding to (111) for samples with compositions of $x = 0.4$, $x = 0.8$ and $x = 1$. Therefore, d spacing of normalized (020) were 0.458 nm, 0.452 nm, 0.446 nm and 0.442 nm, for the four selected samples of $(Na_{1-x}Ca_x)(Sc_{1-x}Mg_x)Si_2O_6:Eu^{2+}$ with $x = 0$, 0.4, 0.8 and 1.0, respectively. In order to verify the relationship of the structure and the composition in this series of samples, Figure S8 gives the d spacings of normalized (020) planes as a function of x values in $(Na_{1-x}Ca_x)(Sc_{1-x}Mg_x)Si_2O_6$ solid-solution series. The excellent linear structural evolution of d-spacings in the (020) planes can be also found in the selected samples with the variation of x values.

Tunable photoluminescence and its application in pc-LEDs. The interesting linear structural evolution of iso-structural $(Na_{1-x}Ca_x)(Sc_{1-x}Mg_x)Si_2O_6$ solid-solution have been found above. However, if the linear behavior of structural parameters is linked with spectroscopic properties, it can be helpful for designing crystal hosts with color-tunable photoluminescence since the changes in spectra can be caused by changes in the Eu^{2+} center environment. In the case of pyroxenes, $CaMgSi_2O_6:Eu^{2+}$ was previously reported as a blue-emitting phosphor and $NaScSi_2O_6:Eu^{2+}$ phosphor shows yellow emission. Therefore, Na environment of Eu^{2+} center leads to spectrum with maximum in yellow region, and Ca environment produce another emission centers in blue region, and the nature on the Eu^{2+} emission and their variation on the emission color will be discussed below. We believe that the variation of blue/yellow emission intensity ratio is expected to be adjusted by the composition value x in

$(Na_{1-x}Ca_x)(Sc_{1-x}Mg_x)Si_2O_6:Eu^{2+}$ solid-solution phosphors. The PL spectra of $(Na_{1-x}Ca_x)(Sc_{1-x}Mg_x)Si_2O_6:0.03Eu^{2+}$ solid-solution phosphors upon 365 nm excitation are shown in Figure 4a. Among them, the activator concentration of Eu^{2+} was fixed at the optimal value (0.03) and the composition of x in $(Na_{1-x}Ca_x)(Sc_{1-x}Mg_x)Si_2O_6$ solid-solution was varied over the range of $x = 0–1$. When $x = 0$, it denotes $NaScSi_2O_6:Eu^{2+}$ phosphor, which exhibits a yellow emission band extending from 410 to 700 nm with a maximum at ~532 nm. With the continuous introduction of $CaMgSi_2O_6$, a blue emission band corresponding to the luminescence of $CaMgSi_2O_6:Eu^{2+}$ phosphor appears and its intensity enhanced with x increasing. Therefore, the as-prepared solid-solution phosphors exhibit a tunable color emission under UV excitation from yellow to blue experiencing the white light emission region. The digital images of some selected phosphors under 365 nm UV lamp are shown in the inset of Figure 4a, and the corresponding visible light emission (yellow $\rightarrow$ white $\rightarrow$ blue color) can be clearly observed with increasing x value. Furthermore, the right inset in Figure 4a shows the PLE of the selected $(Na_{0.7}Ca_{0.3})(Sc_{0.7}Mg_{0.3})Si_2O_6:0.03Eu^{2+}$ sample, and the similar broad excitation bands monitored by two different emission centers, yellow emission center at 532 nm and blue emission at 449 nm, have been clearly found ranging from 200 to 450 nm, which are both ascribed to the transitions of Eu^{2+} between the ground state $4f^7$ and the crystal-field splitted $4f^65d$ configuration[20]. The above spectral results indicate that this series of phosphors can be used as the color-tunable or a single-phase white-emitting phosphor in w-LEDs. We have also measured the absolute quantum efficiency of $(Na_{0.7}Ca_{0.3})(Sc_{0.7}Mg_{0.3})Si_2O_6:0.03Eu^{2+}$ phosphor, and the value is 12.2%. It is found that luminescence efficiency of the solid-solution phase is not high in such a condition; however, we should notice that quantum efficiencies can be modified by the controlling of the phosphor particle size, size distribution, morphology and crystalline defects. The optimization of the luminescence properties can be developed. As an illustration, the EL spectrum of a fabricated w-LED lamp by using single $(Na_{0.7}Ca_{0.3})(Sc_{0.7}Mg_{0.3})Si_2O_6:0.03Eu^{2+}$ phosphor sample and a n-UV LED chip ($\lambda_{ex} = 370$ nm) and the photographs of the w-LED lamp package are demonstrated in the inset of Figure 4b. The EL spectrum clearly shows a n-UV chip emission peak at ~370 nm, a blue emission band at ~454 nm and a yellow emission band at ~537 nm
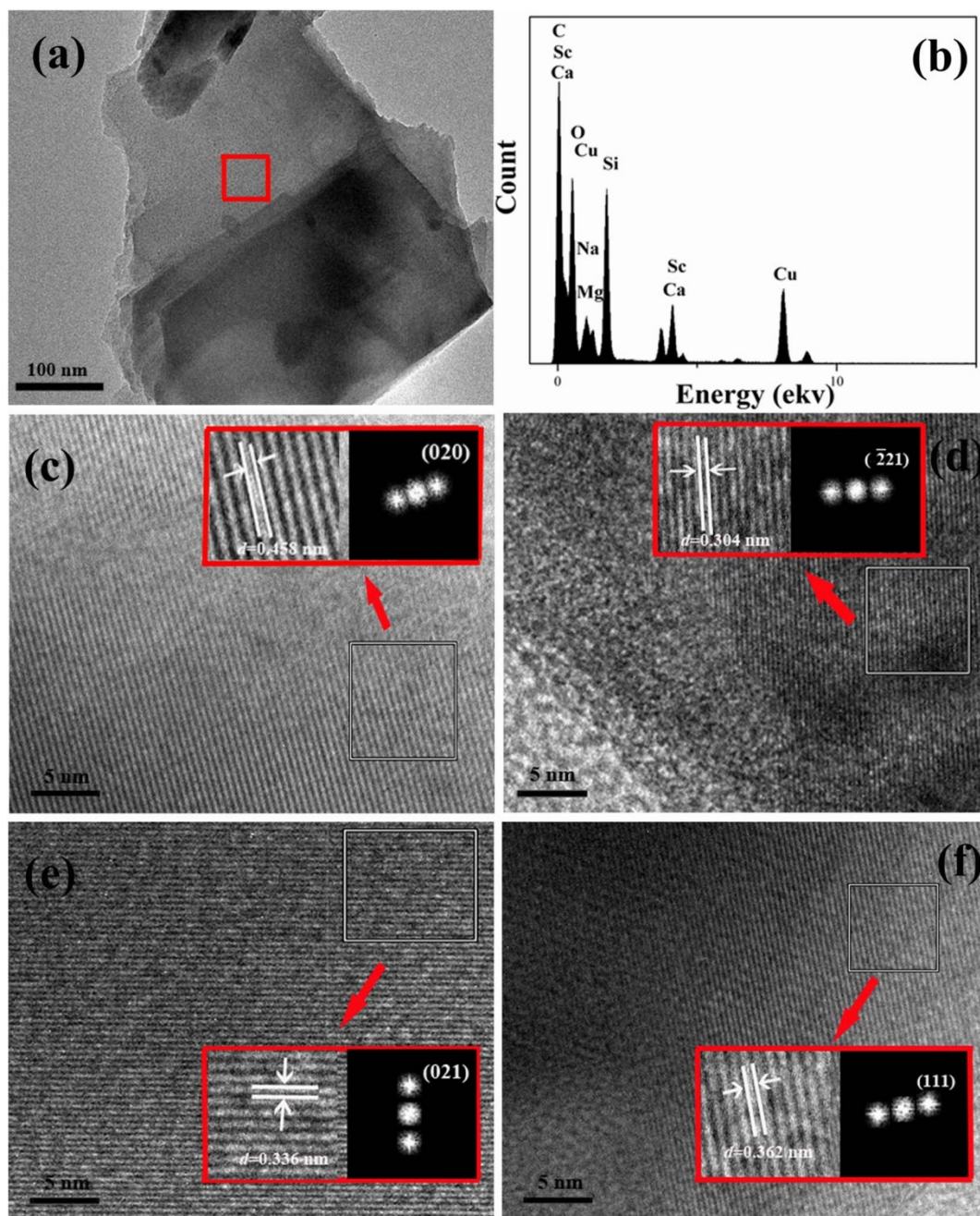
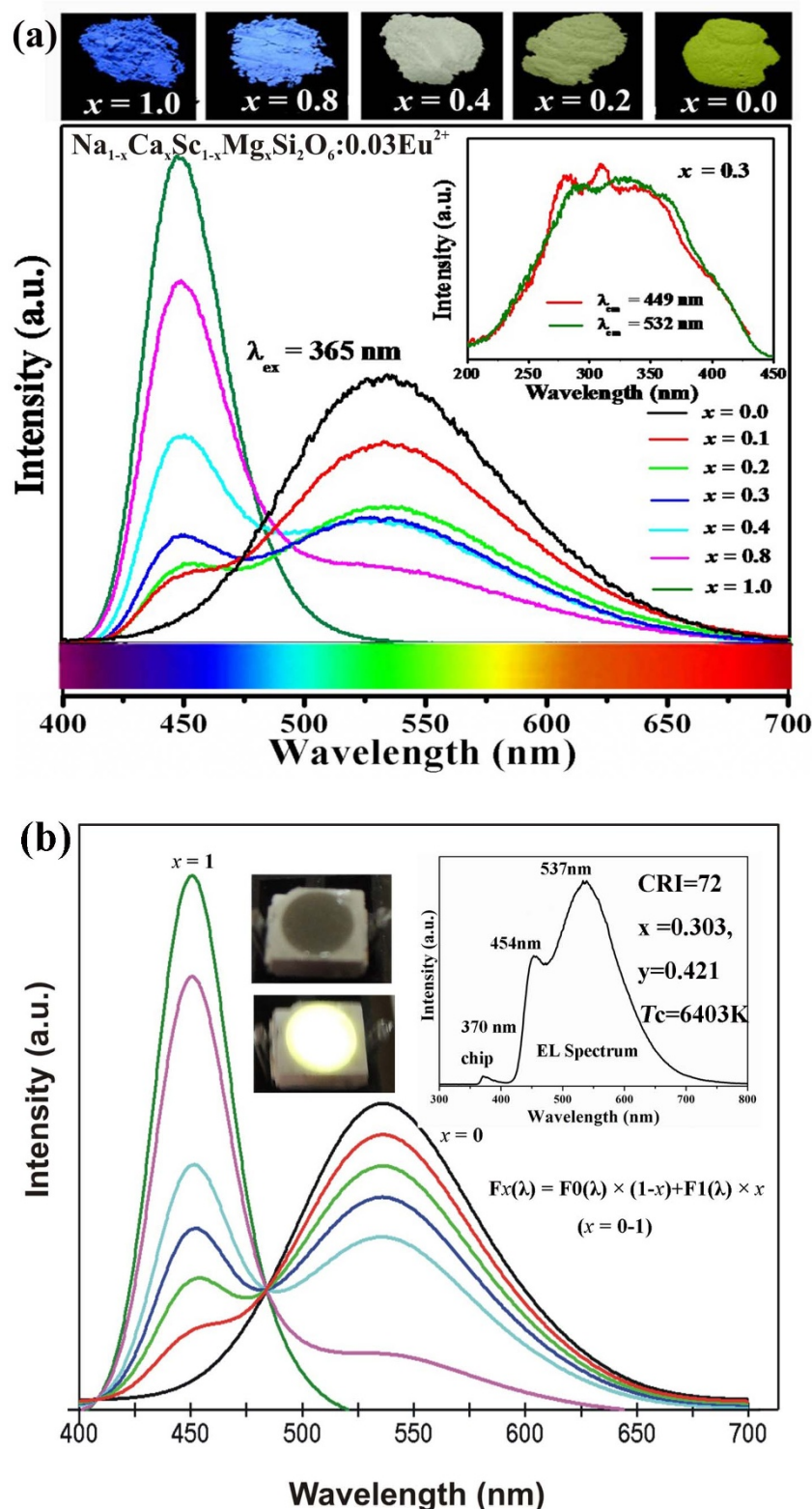**Figure 3** | (a) TEM image of $(Na_{1-x}Ca_x)(Sc_{1-x}Mg_x)Si_2O_6:0.03Eu^{2+}$ ($x = 0.4$) sample, (b) corresponding EDS analysis on a single crystal, and HRTEM images of the selected area for different samples of $(Na_{1-x}Ca_x)(Sc_{1-x}Mg_x)Si_2O_6:0.03Eu^{2+}$ solid-solution series with different x values, $x = 0$ (c), $x = 0.4$ (d), $x = 0.8$ (d) and $x = 1$ (f). The corresponding enlarged lattice fringes and their FFT patterns of the HRTEM images are given in the respective inset.

corresponding to the two different emission centers in $(Na_{0.7}Ca_{0.3})(Sc_{0.7}Mg_{0.3})Si_2O_6:0.03Eu^{2+}$ phosphor. The EL spectral measurement result reveals that CIE color coordinates are (0.303, 0.421) at a cold white light correlated color temperature (CCT) of 6403 K and a CRI value (R_a) is determined as 72. As a newly developed phosphor system, it is believed that its properties can be further explored and optimized to obtain high-quality white light emission in the future research.

Discussion

The above results underline the linear structural evolution of the isostructural $(Na_{1-x}Ca_x)(Sc_{1-x}Mg_x)Si_2O_6$ solid-solutions and the color-tunable emission observed at different x values. That is to say, this series of intermediate compounds do not show substantial changes in structure with any active defect formation, however their spectra can have features from both blue and yellow spectra. We suppose that the additive behavior of spectroscopic properties performs in a similar linear character and the luminescent spectra of the $(Na_{1-x}Ca_x)(Sc_{1-x}Mg_x)Si_2O_6:Eu^{2+}$ solid-solution phosphors can be considered as a superposition of luminescent spectra of $NaScSi_2O_6:Eu^{2+}$ and $CaMgSi_2O_6:Eu^{2+}$. To verify this hypothesis, the spectra of $NaScSi_2O_6:Eu^{2+}$ ($x = 0$) and $CaMgSi_2O_6:Eu^{2+}$ ($x = 1$) in Figure 4a were approximated by functions $F_0(\lambda)$ and $F_1(\lambda)$, respectively. The Gauss function $F(\lambda) = A \times \exp(-(\lambda - \lambda_0)^2/H)$ was used for the approximation. Here λ_0 is the spectral position of individual band maximum in nm. H is proportional to square of

Figure 4 | (a) PL spectra (λ_{ex} = 365 nm) of $(Na_{1-x}Ca_x)(Sc_{1-x}Mg_x)Si_2O_6$:0.03Eu^{2+} solid-solution phosphors with different x values, and the right inset shows the PLE and PL spectra of the selected $(Na_{0.7}Ca_{0.3})(Sc_{0.7}Mg_{0.3})Si_2O_6$:0.03Eu^{2+} sample, and the upper inset gives the digital images of some selected phosphors under 365 nm UV lamp. (b) the calculated spectra of $(Na_{1-x}Ca_x)(Sc_{1-x}Mg_x)Si_2O_6$:0.03Eu^{2+} phosphors by using functions $F_x(\lambda)$ based on the spectra of $NaScSi_2O_6$:0.03Eu^{2+} (x = 0) and $CaMgSi_2O_6$:0.03Eu^{2+} (x = 1) in the linear superposition of functions $F_0(\lambda)$ and $F_1(\lambda)$. The inset gives the EL spectrum of a fabricated w-LED lamp by using $(Na_{0.7}Ca_{0.3})(Sc_{0.7}Mg_{0.3})Si_2O_6$:0.03Eu^{2+} sample and the photographs of the w-LED lamp package.

width of the spectrum. The parameters of $\lambda_0 = 532$ nm, H = 2500 nm² were used for $F_0(\lambda)$ and $\lambda_0 = 449$ nm, H = 500 nm² were used for $F_1(\lambda)$. Parameters A_0 and A_1 were found by least square approximation method. Since peaks of spectra are a little asymmetric it was decided to add one more Gauss function for each $F_0(\lambda)$ and $F_1(\lambda)$. The parameters of this additional function are: $\lambda_0 = 590$ nm, H = 2500 nm² for $F_0(\lambda)$ and $\lambda_0 = 470$ nm, H = 1000 nm² for $F_1(\lambda)$. Final approximation by least square method gives: $F_0(\lambda) = 48.497 \times \exp(-(\lambda - 532)^2/2500) + 12.075 \times \exp(-(\lambda - 590)^2/2500) + 1.635$ and $F_1(\lambda) = 82.567 \times \exp(-(\lambda - 449)^2/500) + 18.587 \times \exp(-(\lambda - 470)^2/1000) - 1.428$. As is shown in Figure 4b, these functions will prove the pints in the measured spectra of $NaScSi_2O_6$:Eu^{2+} ($x = 0$) and $CaMgSi_2O_6$:Eu^{2+} ($x = 1$) shown in Figure 4a. Then, the luminescent spectra of the solid-solution phosphors with intermediated composition were calculated as a superposition of $F_x(\lambda) = F_0(\lambda) \times (1 - x) + F_1(\lambda) \times x$, $(0 \leq x \leq 1)$ based on the linear relationship. The calculated spectra of $(Na_{1-x}Ca_x)(Sc_{1-x}Mg_x)Si_2O_6$:$Eu^{2+}$ solid-solution phosphors by using functions $F_x(\lambda)$ are shown in Figure 4b. The relation between the measured (Figure 4a) and calculated (Figure 4b) spectra is qualitatively good. As is also given in Figure S9, it superimposes the experimental emission curves (shown in Fig. 4a) with the calculated emission curves (shown in Fig. 4b) for $x = 0$, 0.3, and 1.0. The data can clearly prove the points. This result shows that the supposition about the additive behavior of spectroscopic properties is plausible. We also suggest that linear behavior of cell parameters in other compound systems is linked with such additive behavior of spectroscopic properties and can be useful for obtain spectra with predetermined parameters. Evidently, this approach can be developed for other complex solid-solution phosphors.

It is interesting to consider the nature of the emission band superposition in the present solutions $(Na_{1-x}Ca_x)(Sc_{1-x}Mg_x)Si_2O_6$:$Eu^{2+}$. There are two emission bands clearly observed in Figure 4a. Therefore, the existence of two different Eu^{2+} sites may be supposed in the solid solution. Moreover, these two bands are being located at exactly the same position as in the end members. Since two emission bands are still visible in the single phase solid solution, there are two Eu^{2+} sites with different local environment. It is proposed that, in the solid solution all Na^+ ions have to be surrounded by Sc^{3+} ions in order to avoid a local charge mismatch. Likewise, Ca^{2+} ions are surrounded by Mg^{2+} ions. There is still a random distribution of these small NaSc units and CaMg units. But there are local clusters of NaSc and CaMg. That would result in two different Eu^{2+} sites with difference in the covalency, therefore both bands (blue and yellow emission) are still visible in the solid solution explaining the emission spectra we observe.

In conclusion, the new solid-solution phosphors $(Na_{1-x}Ca_x)(Sc_{1-x}Mg_x)Si_2O_6$:$Eu^{2+}$, showing continuously controlled yellow-white-blue emission, are obtained as x increases from 0 to 1. Based on the Rietveld analysis, the unit cell parameters and volumes decrease with increasing relative content of $CaMgSi_2O_6$ in the solid-solution series obeying Vegard's rule of linear relationship, and the excellent linear structural evolution can be also verified by HRTEM examination from the linear variation of d-spacings in the (020) planes with x. The luminescent spectra of the solid-solution phosphors were verified as a superposition of linear mixing by the blue-emitted component ($CaMgSi_2O_6$:Eu^{2+}) and yellow one (NaSc Si_2O_6:Eu^{2+}). The linear behaviour of structural parameters is linked with spectroscopic properties variation and it is helpful for designing color-tunable photoluminescence with predetermined parameters, which will open a window for the study of color-tunable phosphor materials based on the crystal chemistry strategy.

Methods

Sample preparation. All the Eu^{2+} doped $(Na_{1-x}Ca_x)(Sc_{1-x}Mg_x)Si_2O_6$ $(0 \leq x \leq 1)$ solid-solution phosphors were prepared via a sol-gel method. The starting materials of Eu_2O_3 (>99.99%) and $Sc(NO_3)_3$ were supplied by China Minls (Beijing) Research Institute, Beijing, China, and $MnCO_3$ (>99.5%), $NaNO_3$

(>99.5%) and $Si(OC_2H_5)_4$ (>99.5%) were purchased from Sinopharm Chemical Reagent Co. Ltd., Shanghai, China. Briefly, stoichiometric Eu_2O_3 was dissolved in HNO_3 to obtain soluble $Eu(NO_3)_3$, then the stoichiometric amounts of $NaNO_3$, $Ca(NO_3)_2$, $Mg(NO_3)_2$ and $Sc(NO_3)_3$, were added and dissolved in ethanol under stirring. After this, the designed amounts $Si(OC_2H_5)_4$ were added successively in the above solution. The resultant mixtures were stirred at 80°C for 30 min, and homogeneous gels were obtained. After drying at 120°C for 12 h, the dried gels were ground and treated at 800°C for 20 h in the air, and then fully ground and sintered at 1200°C for 5 h in the CO reducing atmosphere. Finally, they were furnace-cooled to room temperature, and fine powders were obtained after grinding.

Structure and optical measurements. Powder X-ray diffraction data were collected by a Panalytical X'pert diffractometer with the Cu Kα radiation at 40 kV and 40 mA. The data for Rietveld analysis were collected in a step-mode with the step size of 0.02° and 20 s counting time per step over the 2θ range from 5° to 130°, and the X-ray beam was controlled by a 0.5° fixed divergence slit. The crystal structure of $NaScSi_2O_6$[15] (JCPDS, 82-0532) was used as a starting model for Rietveld refinement. High resolution transmission electron microscopic (HRTEM) images were characterized by a JEOL JEM-2010 microscope with an accelerated voltage of 200 kV. Photoluminescence excitation (PLE) and emission (PL) spectra were characterized by an F-4600 model fluorescence spectrophotometer with the photomultiplier tube operating at 400 V and the 150 W Xe lamp used as the excitation source. The quantum efficiency (QE) was measured by an Absolute Photoluminescence Quantum Yield Measurement System (C9920-02, Hamamatsu-Photonics) with an integrating sphere at room temperature.

Fabrication of pc-LEDs. The white-light n-UV LED was fabricated using a mixture of silicon resin and the as-prepared white-emitting $(Na_{0.7}Ca_{0.3})(Sc_{0.7}Mg_{0.3})Si_2O_6$: $0.03Eu^{2+}$ sample being dropped onto a 370 nm UV chip. The EL spectrum, R_a, CCT, and CIE value of the lamp, were examined by a PMS-80 Plus UV-Vis-near IR Spectro-photocolorimeter (Everfine, China) instrument.

1. George, N. C., Denault, K. A. & Seshadri, R. Phosphors for Solid-State White Lighting. *Annu. Rev. Mater. Res.* **43**, 2.1–2.21 (2013).
2. Daicho, H. *et al.* A novel phosphor for glareless white light-emitting diodes. *Nature Commun.* **3**, 1132–1139 (2012).
3. Bachmann, V., Ronda, C. & Meijerink, A. Temperature Quenching of Yellow Ce^{3+} Luminescence in YAG:Ce. *Chem. Mater.* **21**, 2077–2084 (2009).
4. Setlur, A. A. *et al.* Crystal Chemistry and Luminescence of Ce^{3+}-Doped $Lu_2CaMg_2(Si, Ge)_3O_{12}$ and Its Use in LED Based Lighting. *Chem. Mater.* **18**, 3314–3322 (2006).
5. Shang, M. M. *et al.* J. Tunable Luminescence and Energy Transfer properties of Sr_3AlO_4F:RE^{3+} (RE = Tm/Tb, Eu, Ce) Phosphors. *ACS Appl. Mater. Interfaces* **3**, 2738–2746 (2011).
6. Xia, Z. G., Wang, X. M., Wang, Y. X., Liao, L. B. & Jing, X. P. Synthesis, structure, and thermally stable luminescence of Eu^{2+}-doped $Ba_2Ln(BO_3)_2Cl$ (Ln = Y, Gd and Lu) host compounds. *Inorg. Chem.* **50**, 10134–10142 (2011).
7. Huang, C. H. *et al.* A single-phased emission-tunable phosphor $Ca_9Y(PO_4)_7$:Eu^{2+},Mn^{2+} with efficient energy transfer for white-light-emitting diodes. *ACS Appl. Mater. Interfaces.* **2**, 259–264 (2010).
8. Li, G. G. *et al.* Tunable luminescence of Ce^{3+}/Mn^{2+}-coactivated $Ca_2Gd_8(SiO_4)_6O_2$ through energy transfer and modulation of excitation: potential single-phase white/yellow-emitting phosphors. *J. Mater. Chem.* **21**, 13334–13344 (2011).
9. Lu, W. *et al.* Tunable full-color emitting $BaMg_2Al_6Si_9O_{30}$:Eu^{2+},Tb^{3+},Mn^{2+} phosphors based on energy transfer. *Inorg. Chem.* **50**, 7846–7851 (2011).
10. Martínez-Martínez, R., Álvarez, E., Speghini, A., Falcony, C. & Caldiño, U. White light generation in Al_2O_3:Ce^{3+}:Tb^{3+}:Mn^{2+} films deposited by ultrasonic spray pyrolysis. *Thin Solid Films.* **518**, 5724–5730 (2010).
11. Burns, R. G. *Mineralogical Applications of Crystal Field Theory*, 2nd edition [Burns, R. G. (ed.)] (Cambridge University Press, Cambridge, 1993).
12. Jiang, L., Chang, C., Mao, D. & Feng, C. Luminescent properties of $CaMgSi_2O_6$-based phosphors co-doped with different rare earth ions. *J. Alloy Compd.* **377**, 211–215 (2004).
13. Xia, Z. G., Zhang, Y. Y., Molokeev, M. S. & Atuchin, V. V. Structural and Luminescence Properties of Yellow-Emitting $NaScSi_2O_6$:Eu^{2+} Phosphors: Eu^{2+} Site Preference Analysis and Generation of Red Emission by Codoping Mn^{2+} for White-Light-Emitting Diode Applications. *J. Phys. Chem. C.* **117**, 20847–20854 (2013).
14. Hawthorne, F. C. & Grundy, H. D. Refinement of the crystal structure of $NaScSi_2O_6$. *Acta Cryst.* **B29**, 2615–2616 (1973).
15. Ohashi, H., Osawa, T. & Sato, A. $NaScSi_2O_6$. *Acta Cryst C* **50**, 838–840 (1994).
16. Smallman, R. E. *Modern Physical Metallurgy*, 4th Edition, [Smallman, R. E. (ed.)] (Butterworths, London, 1985).
17. Shannon, R. D. Revised effective ionic radii and systematic studies of interatomic distances in halides and chalcogenides. *Acta. Cryst A* **32**, 751–767 (1976).
18. Mellini, M., Merlino, S., Orlandi, P. & Rinaldi, R. Cascandite and jervisite, two new scandium silicates from Baveno, Italy. *Am. Mineral.* **67**, 599–603 (1982).
19. Cullity, B. D. & Stock, S. R. *Elements of x-ray diffraction*, 3rd edition, [Cullity, B. D., Stock, S. R. (ed.)] (Prentice Hall, New Jersey, 2003).

20. Blasse, G. & Grabmaier, B. C. *Luminescent Materials* [Blasse, G., Grabmaier, B. C. (ed.)] (Springer-Verlag, Berlin, 1994).

Author contributions

Z.X. proposed the idea of this experimental design, carried out XRD measurements, fabricated pc-LEDs and wrote the paper. Y.Z. synthesized materials and performed the spectral measurement. M.M. carried out the structural analysis and spectral mixing calculation. V.A. participated in discussions of the data and the revision of the paper. Y.L. performed the TEM measurement. All authors reviewed the manuscript.

Additional information

Supplementary information accompanies this paper at http://www.nature.com/scientificreports

Competing financial interests: The authors declare no competing financial interests.

How to cite this article: Xia, Z.G., Zhang, Y.Y., Molokeev, M.S., Atuchin, V.V. & Luo, Y. Linear structural evolution induced tunable photoluminescence in clinopyroxene solid-solution phosphors. *Sci. Rep.* **3**, 3310; DOI:10.1038/srep03310 (2013).